

Investigation of Two-Dimensional Vibrational Spectrum by a Diagrammatic Approach

Keisuke Tominaga* and Hiroaki Maekawa

Department of Chemistry, Faculty of Science, Kobe University, Nada, Kobe, 657-8501

(Received August 11, 2000)

We have theoretically investigated two-dimensional vibrational spectra for a two-mode system in terms of a diagrammatic approach. The two vibrational modes are anharmonically coupled. The perturbed stationary states are obtained by treating the cubic anharmonicity as a perturbation, and expressions for the third order response functions are derived. A physical origin of cross peaks in the spectrum is discussed. It is found that the vibrational dephasing time as well as the anharmonicity is important for the appearance of cross peaks.

The development of optical two-dimensional (2D) spectroscopy is one of the major topics in the field of the current ultrafast laser spectroscopy.[1–22] Optical 2D spectroscopy is an optical analogue of the 2D magnetic resonance technique, which permits the resolution of congested spectra by spreading them out into the frequency dimensions. In principle, the basic idea of 2D NMR[23] can be applied to any quantum-mechanical two-level system, such as vibrational and electronic states. For this decade, 2D vibrational and electronic spectroscopies have been developed theoretically and experimentally. These techniques are expected to be capable of providing novel information in condensed phases, such as a correlation among the states and the dynamics in the states.

In this article we theoretically investigate the spectral pattern of 2D vibrational spectroscopy in terms of a diagrammatic approach. From an analogy of 2D NMR technique, it is expected that a cross peak between two vibrational modes may be observed if these two modes are correlated in some way. If there is no correlation between the modes, peaks will be observed only along the diagonal line in the 2D spectrum. Therefore, one basic question on vibrational 2D spectroscopy is what kind of conditions are necessary for the observation of cross peaks, and how large are the intensities of the cross peaks compared to those of the peaks along the diagonal line. Theoretical investigations have been made on the two-dimensional vibrational spectra by Mukamel and coworkers,[6,7] Tanimura and Okumura,[12] and Cho and coworkers.[15] They have especially studied the 2D spectra of the fifth ($x^{(5)}$) and the seventh ($x^{(7)}$) order electronically off-resonant Raman spectroscopies. They have shown that cross peaks may result from either intermode coupling via diagonal elements of polarizability or anharmonic intermode coupling.[7,12] In this work we investigated the 2D vibrational spectra by constructing perturbed stationary states and treating fluctuation of the transition frequencies in terms of stochastic theory.[22]

During the course of this study Hochstrasser and coworkers have reported the first 2D IR spectrum experimentally obtained for peptides.[21] The experiment which is explained in this work is the same as theirs.

1. Two-Dimensional Vibrational Spectroscopy

Here, we consider three-pulse heterodyne-detected photon echo experiments with IR short pulses. The pulse scheme and a schematic picture of the experiment are shown in Fig. 1. These methods are an optical analogue of NOESY (nuclear Overhauser effect spectroscopy) of the magnetic resonance technique. During the first time interval (t_1), the system is in the coherent state, which is followed by the evolution period of the diagonal state during T. The system is again changed to a coherent state by the third excitation at $t_1 + T$. The photon echo signal results from an induced third-order nonlinear polarization and appears at the phase-matching direction, $\boldsymbol{k}_s = -\boldsymbol{k}_1 + \boldsymbol{k}_2 + \boldsymbol{k}_3$, where $\boldsymbol{k}_i$ is the wavevector of the i-th pulse, and $\boldsymbol{k}_s$ the wavevector of the photon echo signal. A time profile of the echo signal is detected by a gating pulse $\boldsymbol{k}_g$ at $t_1 + T + t_2$ in a heterodyne way. The signal intensity is measured as a function of t_1 and t_2 with a fixed value of T. By performing a double Fourier transform with respect to t_1 and t_2, a 2D spectrum is constructed.

In this work, the time evolution of the system is discussed in terms of the perturbed stationary states, which are solutions of the time-independent Schrödinger equation by treating anharmonicity as a perturbation. Optical transitions between the stationary states are considered, and the time dependence of the diagonal and off-diagonal elements of the density matrix evaluated. This approach has often been used to solve static and dynamic problems in vibrational spectroscopy.[8,19,22,24,25] Another approach to trace the time evolution of the system is to solve the Liouville equation for the density matrix whose basis set is unperturbed states within the framework of the perturbation theory. In this case, the unperturbed states are for a harmonic oscillator. This type of approach has normally been used to

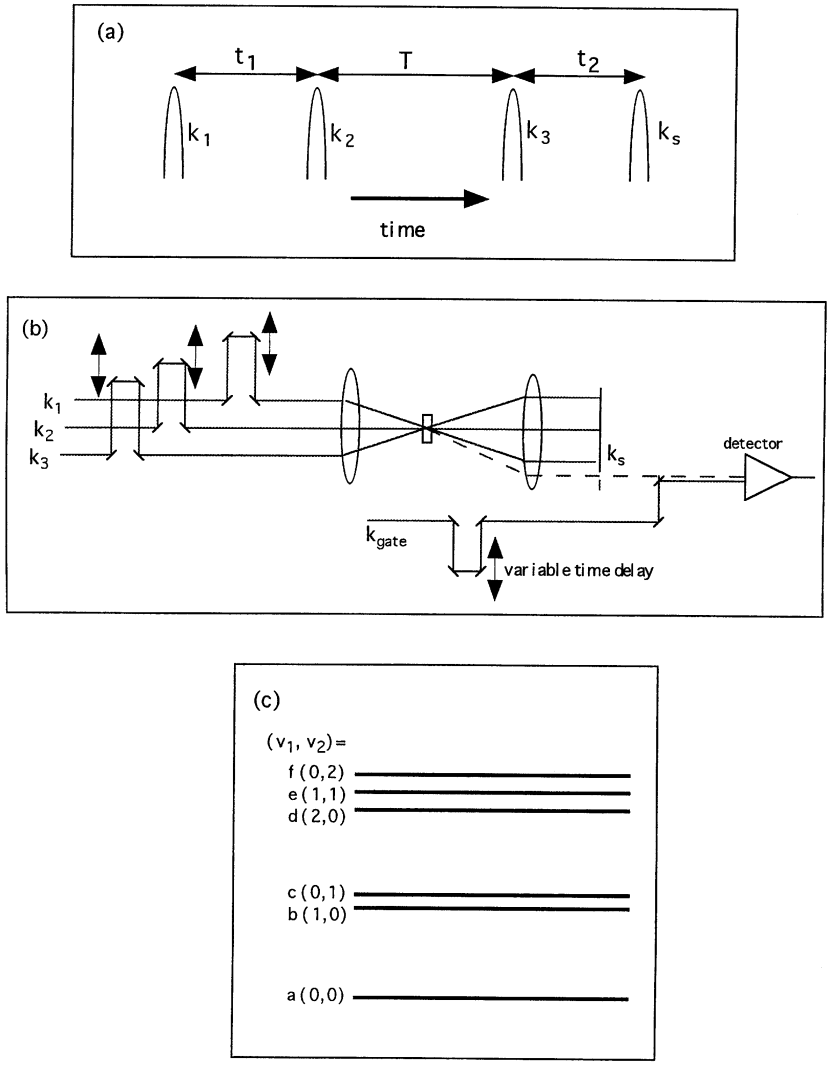

Fig. 1. (a) A pulse scheme for two-dimensional optical spectroscopy. (b) A schematic picture of the heterodyne-detected three pulse photon echo experiment. (c) An energy level diagram for the two vibrational mode case.

solve various problems in magnetic resonance[26] and optical nonlinear spectroscopy.[27]

We consider a model system with two vibrational modes having close, but different, transition frequencies to see how the vibrational correlation appears in the 2D spectrum. Accordingly, it is assumed that the input optical pulse is spectrally so broad that several vibrational levels are coherently excited. Figure 1(c) shows a schematic picture of six quantum states which should be taken into account in the case of 2D vibrational spectroscopy for a two-mode system. Here, we have to pay attention to a possible contribution of the $v = 2$ state as well as the $v = 0$ and $v = 1$ states. If the anharmonicity is sufficiently weak compared to the spectral width of the excitation pulse, the interaction with the second or third pulse may create coherence between the $v = 1$ and $v = 2$ states. Here, we focus on the frequency range around the fundamental transition; therefore, the following eight transition frequencies must be considered: ω_{ba}, ω_{ca}, ω_{db}, ω_{dc}, ω_{eb}, ω_{ec}, ω_{fb}, and ω_{fc}.

2. Calculation of Two-Dimensional Spectrum

2.1. A Diagrammatic Approach. Our approach to evaluate the time evolution of the system is similar to the standard method,[8,19,22,24,25] in which we construct all possible quantum pathways contributing to the third-order polarization and calculate a response function for each quantum pathway. Figure 2 shows all of the diagrams to be considered. For simplicity, we here restrict ourselves to a pulse sequence with all positive time delays ($t_1 > 0$, $T > 0$, $t_2 > 0$). The time evolution of the density matrix is illustrated in terms of the Lee–Albrecht ladder diagram[28] in each diagram, where the solid and broken lines correspond to the action of the electromagnetic field to the bra and ket states, respectively. All of the diagrams survive the rotating wave approximation, since the bandwidth of the pulses is assumed to be much smaller than their center frequency. It is interesting to see that, even during the second time period T, the system is in a coherent state, as shown in, for example, diagram (7) or (8) in Fig. 2, though this time duration is some-

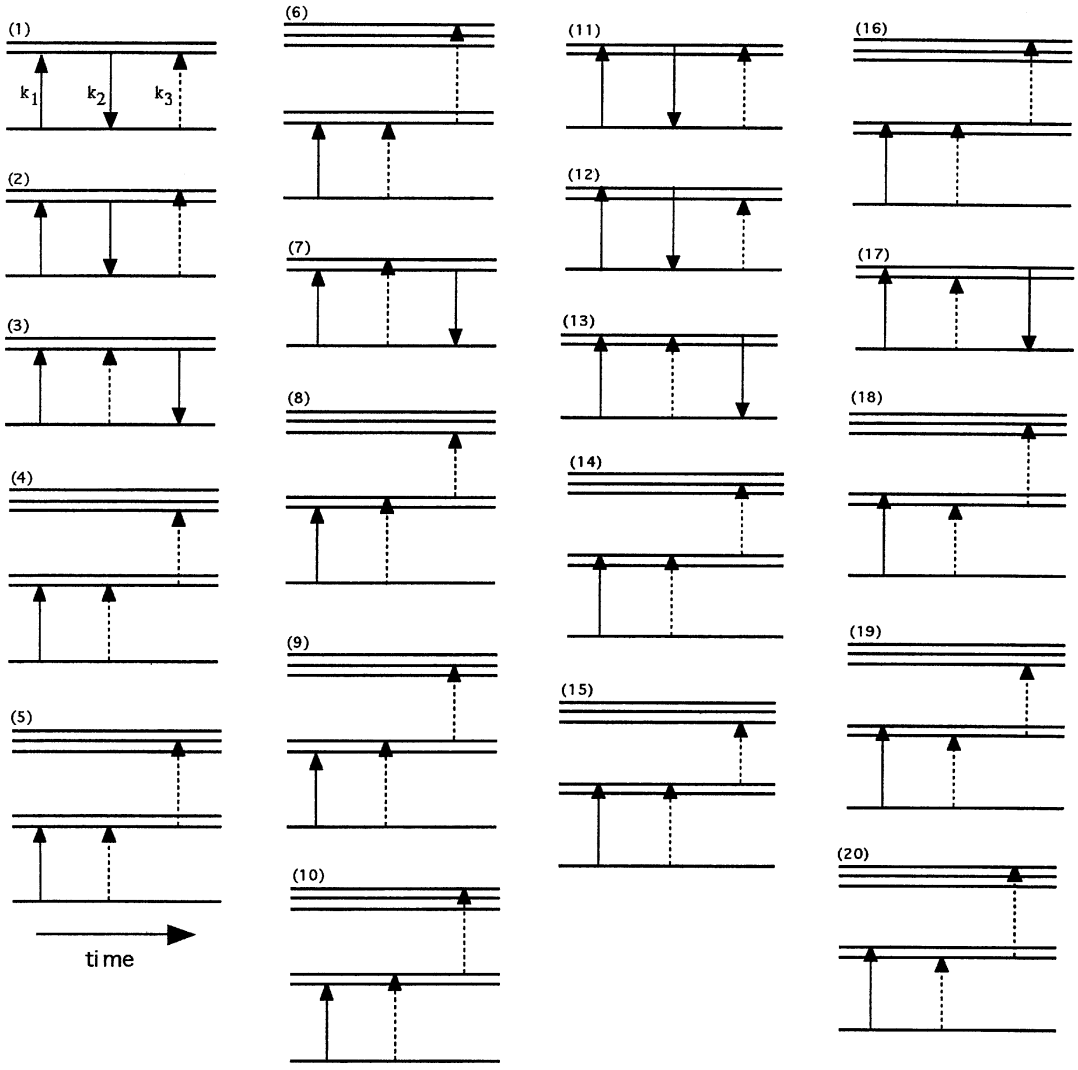

Fig. 2. The 20 quantum pathways for two-dimensional vibrational spectroscopy.

times called a "population period" or "diagonal period". These names are adequate only for a one-mode case.

We further assume $T = 0$ to simplify the model. An extension to the general three-pulse photon echo experiment with $T \neq 0$ is feasible. Each quantum pathway has a corresponding response function, expressed as[1,18,22]:

$$R_i^{(3)}(t_1,t_2) \propto \varepsilon\mu_1\mu_2\mu_3\mu_s \exp(-i\omega_{kl}t_1 - i\omega_{mn}t_2) \left\langle \exp\left\{ -i\int_0^{t_1} \Delta\omega_{kl}(\tau)\mathrm{d}\tau - i\int_{t_1}^{t_1+t_2} \Delta\omega_{mn}(\tau)\mathrm{d}\tau \right\} \right\rangle, \quad (1)$$

where the Born–Oppenheimer approximation is employed, and during the first time interval (t_1) the density matrix of the system is ρ_{kl}, and the during the third time interval (t_2) the density matrix is ρ_{mn}.

$$\omega_{kl} = (E_k - E_l)/\hbar, \quad (2)$$

$\alpha\nu\delta\mu_i$ is the transition dipole moment associated with the i-th pulse, and s denotes the signal. $\varepsilon = 1$ (–1) when the number of action of the electromagnetic field to the ket state is even (odd).

The parentheses in Eq. 1, $\langle\cdots\rangle$, denote the ensemble average in the equilibrium states and can be expanded in terms of the line shape function, $g_{kl,mn}(t)$,

$$\left\langle \exp\left\{ -i\int_0^{t_1} \Delta\omega_{kl}(\tau)\mathrm{d}\tau - i\int_{t_1}^{t_1+t_2} \Delta\omega_{mn}(\tau)\mathrm{d}\tau \right\} \right\rangle = \exp(-g_{kl,kl}(t_1) - g_{mn,mn}(t_2) + g_{kl,mn}(t_1) + g_{kl,mn}(t_2) - g_{kl,mn}(t_1+t_2)), \quad (3)$$

where

$$g_{kl,mn}(t) = \int_0^t \mathrm{d}\tau_1 \int_0^{\tau_1} \mathrm{d}\tau_2 \langle \Delta\omega_{kl}(\tau_1)\Delta\omega_{mn}(\tau_2)\rangle. \quad (4)$$

The third-order polarization is evaluated by convoluting the response function, $\sum_i R_i(t_1, t_2, t_3)$, with the electromagnetic fields of the three excitation pulses. The intensity of the heterodyne-detected signal is proportional to the polarization.

A central issue of the present problem is how to evaluate the response function, Eq. 1, which consists of three factors: the transition dipole moment term $\varepsilon\mu_1\mu_2\mu_3\mu_s$, the oscillating term

or transition frequency term exp ($-i\omega_{kl}t_1 - i\omega_{mn}t_2$), and the term of the time correlation function of the transition frequency fluctuations. In the following sections, we consider these three factors independently.

2.2. Energy Levels and Wavefunctions of Anharmonic Oscillators. First, the energy levels and wavefunctions are obtained for the two-mode case. Most models for vibrational dephasing begin with a common perturbation approach to a solvent–solute interaction. The vibrational Hamiltonian for a molecule interacting with a bath is written as,

$$H_{tot}(t) = H_h + H_{anh} + H_c(t). \tag{5}$$

Here, $H_h + H_{anh}$ is the Hamiltonian for an isolated molecule, H_h is the harmonic part of the Hamiltonian, and H_{anh} is an anharmonic term,

$$H_h = \frac{1}{2m_1}p_1^2 + \frac{1}{2}m_1\omega_1^2x_1^2 + \frac{1}{2m_2}p_2^2 + \frac{1}{2}m_2\omega_2^2x_2^2, \tag{6}$$

$$H_{anh} = \frac{1}{6}f_{111}x_1^3 + \frac{1}{6}f_{112}x_1^2x_2 + \frac{1}{6}f_{122}x_1x_2^2 + \frac{1}{6}f_{222}x_2^3, \tag{7}$$

where we assume a molecule with two vibrational modes which are coupled by a weakly anharmonic interaction, and m_1 (m_2) is the reduced mass, ω_1 (ω_2) the harmonic frequency, x_1 (x_2) the displacement from equilibrium internuclear separation, p_1 (p_2) the momentum conjugated to x_1 (x_2) of the mode 1 (2). f_{ijk} is the cubic anharmonicity. We ignore the second-order coupling between the two modes ($k_{12}x_1x_2$) since the coordinates can be expressed so that the second-order coupling is zero. The solvent–oscillator interaction ($H_c(t)$) is expanded in the oscillator coordinates up to the second order,

$$\begin{aligned} H_c(t) = {} & \left.\frac{\partial V}{\partial x_1}\right|_{x_1=x_1^0} x_1 + \left.\frac{\partial V}{\partial x_2}\right|_{x_2=x_2^0} x_2 + \left.\frac{\partial^2 V}{\partial x_1 \partial x_2}\right|_{x_1=x_1^0, x_2=x_2^0} x_1x_2 \\ & + \left.\frac{\partial^2 V}{\partial x_1^2}\right|_{x_1=x_1^0} x_1^2 + \left.\frac{\partial^2 V}{\partial x_2^2}\right|_{x_2=x_2^0} x_2^2 \\ = {} & F_1(t)x_1 + F_2(t)x_2 + G_{12}(t)x_1x_2 + G_{11}(t)x_1^2 + G_{22}(t)x_2^2. \end{aligned} \tag{8}$$

Madden and Lyden–Bell[24] and Oxtoby and Rice[25] showed that the vibrational dephasing is determined by population relaxation in the case of a harmonic oscillator with a solvent-solute interaction up to the first order in the oscillator coordinate. For polyatomic molecules in liquids, vibrational dephasing is generally faster than population relaxation. Therefore, anharmonicity and the second-order coupling in the solvent-oscillator interaction are intrinsic in the vibrational dephasing of liquids.

The energy levels and wavefunctions for the harmonic Hamiltonian are written in the following way:

$$H_h(\psi_\xi^1\psi_\eta^2) = (E_\xi^2 + E_\eta^2)(\psi_\xi^1\psi_\eta^2) \tag{9}$$

and

$$\left(\frac{1}{2m}p_i^2 + \frac{1}{2}m_i\omega_i^2x_i^2\right)\psi_\xi^i = E_\xi^i\psi_\xi^i. \tag{10}$$

The wavefunctions for the anharmonic oscillators are expressed by a linear combination of a basis set for a harmonic oscillator,

$$\Phi_{mn} = \sum c_{mn,\xi\eta}\psi_\xi^1\psi_\eta^2 \tag{11}$$

The usual procedure is to first solve for the eigenstates of H_h+H_{anh} in terms of the eigenstates for a harmonics oscillator $\{|\xi\eta>\}$ by treating the anharmonicity as a perturbation. It should be noted that the states denoted by ξ and η correspond to a harmonic oscillator, but the states denoted by m and n are no longer for a harmonic oscillator. Solving the equation by first-order perturbation theory, it is found that non-zero coefficients of $c_{mn,\xi\eta}$ are on the order of $(\gamma_i^3 f_{jkl}/\varepsilon_m)$, where

$$\gamma_i = \sqrt{\frac{\hbar}{2m_i\omega_i}} \quad \text{and} \quad \varepsilon_i = \hbar\omega_i \tag{12}$$

2.3. Transition Dipole Moments. The optical transition from the initial state with a wavefunction Φ_{mn} to the final state with a wavefunction Φ_{ij} can be described by a transition dipole moment ($\mu_{mn,ij}$),

$$\mu_{mn,ij} = \left\langle \Phi_{mn} \left| \tilde{r} \right| \Phi_{ij} \right\rangle = \mu^0_{mn,ij} + \sum_{\xi\eta,\zeta\theta} c_{mn,\xi\eta}c^*_{ij,\zeta\theta}\mu^0_{\xi\eta,\zeta\theta} \tag{13}$$

Here, $\tilde{r}$ is the dipole transition operator and $\mu^0_{\xi\eta,\zeta\theta}$ is the transition dipole for the harmonic approximation. The additional term, $\sum_{\xi\eta,\zeta\theta} c_{mn,\xi\eta}c^*_{ij,\zeta\theta}\mu^0_{\xi\eta,\zeta\theta}$, describes a deviation from the harmonic approximation due to anharmonicity. We do not consider here the influence of orientational relaxation on the third-order polarization. In order to include the effect, a correlation function for orientational diffusion should be calculated for the $x^{(3)}$ tensor elements relevant to isotropic media.

2.4. Transition Frequencies. For anharmonic oscillators, the energy levels of the vibrational states are empirically expressed as

$$\begin{aligned} \frac{E_{mn}}{\hbar} = {} & \kappa_1\left(m+\frac{1}{2}\right) + \kappa_2\left(n+\frac{1}{2}\right) + \kappa_{11}\left(m+\frac{1}{2}\right)^2 \\ & + \kappa_{22}\left(n+\frac{1}{2}\right)^2 + \kappa_{12}\left(m+\frac{1}{2}\right)\left(n+\frac{1}{2}\right) + \end{aligned} \tag{14}$$

The empirical spectroscopic parameters, such as κ_1 or κ_{22}, are expressed in terms of the parameters in the Hamiltonian, such as the cubic anharmonicities.[30]

2.5. Time Correlation Functions. The time-dependent transition frequency between the vibrational states ($v_1 = m$, $v_2 = n$, abbreviated as (mn)) and (ij) is expressed as

$$\begin{aligned} \Delta\omega_{mn,ij}(t) &= \frac{1}{\hbar}\left[\int \mathrm{d}r\Phi^*_{mn}H_c(t)\Phi_{mn} - \int \mathrm{d}r\Phi^*_{ij}H_c(t)\Phi_{ij}\right] \\ &= \frac{1}{\hbar}[\langle mn|H_c(t)|mn\rangle - \langle ij|H_c(t)|ij\rangle] \end{aligned} \tag{15}$$

Here, the eight time-dependent transition frequencies ($\Delta\omega_{ba}(t)$, $\Delta\omega_{ca}(t)$, $\Delta\omega_{db}(t)$, $\Delta\omega_{dc}(t)$, $\Delta\omega_{eb}(t)$, $\Delta\omega_{ec}(t)$, $\Delta\omega_{fb}(t)$, and $\Delta\omega_{fc}(t)$) must be evaluated. In order to evaluate the above quantities, the following matrix element of the time-dependent solvent-oscillator interaction should be calculated:

$$\langle mn|H_c(t)|mn\rangle = \sum_{\xi\eta,\zeta\theta} c^*_{mn,\xi\eta}c_{mn,\zeta\theta}\int \mathrm{d}r\left(\psi_\xi^1\psi_\eta^2\right)^* H_c(t)\left(\psi_\zeta^1\psi_\theta^2\right) \tag{16}$$

Consequently,

$$\begin{aligned}
&\langle mn|H_c(t)|mn\rangle \\
&= \sum_{\xi,\eta} \gamma_1 F_1(t)\Big(\sqrt{\xi+1}c^*_{mn,\xi+1\eta}c_{mn,\xi\eta} + \sqrt{\xi}c^*_{mn,\xi-1\eta}c_{mn,\xi\eta}\Big) \\
&+ \gamma_2 F_2(t)\Big(\sqrt{\eta+1}c^*_{mn,\xi\eta+1}c_{mn,\xi\eta} + \sqrt{\eta}c^*_{mn,\xi\eta-1}c_{mn,\xi\eta}\Big) \\
&+ \gamma_1\gamma_2 G_{12}(t)\Big(\sqrt{\xi+1}\sqrt{\eta+1}c^*_{mn,\xi+1\eta+1}c_{mn,\xi\eta} \\
&+ \sqrt{\xi+1}\sqrt{\eta}c^*_{mn,\xi+1\eta-1}c_{mn,\xi\eta} \\
&+ \sqrt{\xi}\sqrt{\eta+1}c^*_{mn,\xi-1\eta+1}c_{mn,\xi\eta} \\
&+ \sqrt{\xi}\sqrt{\eta}c^*_{mn,\xi-1\eta-1}c_{mn,\xi\eta}\Big) \\
&+ \gamma_1^2 G_{11}(t)\Big(\sqrt{\xi+1}\sqrt{\xi+2}c^*_{mn,\xi+2\eta}c_{mn,\xi\eta} \\
&+ (2\xi+1)c^*_{mn,\xi\eta}c_{mn,\xi\eta} + \sqrt{\xi}\sqrt{\xi-1}c^*_{mn,\xi-2\eta}c_{mn,\xi\eta}\Big) \\
&+ \gamma_2^2 G_{22}(t)\Big(\sqrt{\eta+1}\sqrt{\eta+2}c^*_{mn,\xi\eta+2}c_{mn,\xi\eta} \\
&+ (2\eta+1)c^*_{mn,\xi\eta}c_{mn,\xi\eta} + \sqrt{\eta}\sqrt{\eta-1}c^*_{mn,\xi\eta-2}c_{mn,\xi\eta}\Big) \qquad (17)
\end{aligned}$$

By using the above equations, the diagonal elements of the Hamiltonian are estimated as, for example,

$$\begin{aligned}
\langle 00|H_c(t)|00\rangle &= \frac{\gamma_1^2 F_1(t)}{\varepsilon_1}\left(\gamma_1^2 f_{111} + \frac{1}{3}\gamma_2^2 f_{122}\right) \\
&+ \frac{\gamma_2^2 F_2(t)}{\varepsilon_2}\left(\frac{1}{3}\gamma_1^2 f_{112} + \gamma_2^2 f_{222}\right) \\
&+ \gamma_1^2 G_{11}(t) + \gamma_2^2 G_{22}(t). \qquad (18)
\end{aligned}$$

Finally, the expressions are obtained for the fluctuations of the transition frequencies. One example is

$$\begin{aligned}
\hbar\Delta\omega_{ba}(t) &= \langle 10|H_c(t)|10\rangle - \langle 00|H_c(t)|00\rangle \\
&= \frac{2\gamma_1^4 f_{111}}{\varepsilon_1}F_1(t) + \frac{2\gamma_1^2\gamma_2^2 f_{112}}{3\varepsilon_2}F_2(t) + 2\gamma_1^2 G_{11}(t) \qquad (19)
\end{aligned}$$

The other seven expressions for the frequency fluctuations are given in Appendix. The time correlation functions of the frequency fluctuations are evaluated, for example,

$$\begin{aligned}
\langle\Delta\omega_{ba}(t)\Delta\omega_{ba}(0)\rangle &= \frac{4\gamma_1^8 f_{111}^2}{\hbar^2\varepsilon_1^2}\langle F_1(t)F_1(0)\rangle \\
&+ \frac{4\gamma_1^4\gamma_2^4 f_{112}^2}{9\hbar^2\varepsilon_2^2}\langle F_2(t)F_2(0)\rangle \\
&+ 4\frac{\gamma_1^4}{\hbar^2}\langle G_{11}(t)G_{11}(0)\rangle, \qquad (20)
\end{aligned}$$

$$\begin{aligned}
\langle\Delta\omega_{ba}(t)\Delta\omega_{ca}(0)\rangle &= \langle\Delta\omega_{ca}(t)\Delta\omega_{ba}(0)\rangle \\
&= \frac{4\gamma_1^6\gamma_2^2 f_{111}f_{122}}{3\hbar^2\varepsilon_1^2}\langle F_1(t)F_1(0)\rangle \\
&+ \frac{4\gamma_1^2\gamma_2^6 f_{112}f_{222}}{3\hbar^2\varepsilon_2^2}\langle F_2(t)F_2(0)\rangle \qquad (21)
\end{aligned}$$

Here, we invoke the classical approximation[26] and assume the following relations:

$$\begin{aligned}
&\langle F_i(t)F_j(0)\rangle \ll \langle F_i(t)F_i(0)\rangle \quad \text{and} \\
&\langle G_{ii}(t)G_{jj}(0)\rangle \ll \langle G_{ii}(t)G_{ii}(0)\rangle \quad \text{if} \quad i \neq j, \qquad (22)
\end{aligned}$$

where the time-correlation functions between $F_i(t)$ and $G_{ii}(t)$ or $G_{jj}(t)$ are negligible. The coefficients for the $G_{ii}(t)$ and $G_{jj}(t)$ terms do not contain the anharmonicity constants ($f_{111}, f_{112}, f_{122}$, f_{222}). The coefficients for the $F_i(t)$ terms carry information on the anharmonicity. It is interesting to notice that the time-correlation function for the cross term, $\langle\Delta\omega_{ba}(t)\Delta\omega_{ca}(0)\rangle$ in Eq. 21 consists of two terms, both of which include the cross anharmonicities, f_{112} or f_{122}. On the other hand, the time-correlation function for the diagonal term, $\langle\Delta\omega_{ba}(t)\Delta\omega_{ba}(0)\rangle$, in Eq. 20, has a term with only the "diagonal" anharmonicity (f_{111} and f_{222}). Considering that the diagonal anharmonicities, f_{111} and f_{222}, are normally much greater than the cross anharmonicities, f_{112} and f_{122}, for organic molecules, the coefficients in Eq. 21, such as $(4\gamma_1^6\gamma_2^2 f_{111}f_{122}/3\hbar^2\varepsilon_1^2)$, are much smaller than those in Eq. 20, such as $(4\gamma_1^8 f_{111}^2/\hbar\varepsilon_1^2)$.

3. Two-Dimensional Spectrum.

In this chapter we investigate the spectral pattern of the 2D vibrational spectrum. Figure 3 is a schematic picture which illustrates the diagonal and off-diagonal (cross) peaks in the 2D spectrum resulting from the 20 diagrams in Fig. 2. In this picture we assume that the four cubic anharmonicities (f_{111}, f_{112}, f_{122}, and f_{222}) are not zero. Then, all eight transition frequencies have different values. Cross peaks, such as (ω_{ba}, $-\omega_{ca}$) and (ω_{ca}, $-\omega_{ba}$), appear in the spectrum, as we expected for an anharmonically-coupled two-mode case. It should be noticed that there are, in principle, ten different peaks in the 2D spectrum, even for the two-mode case. Each peak is named with a capital alphabet. The numbers in parentheses above the peaks correspond to the diagrams in Fig. 2. Each peak has a sign (+ or –) depending on the phase of the polarization.

3.1. Spectral Shape and Intensities of the Peak. We discuss the line shape of the 2D spectrum first. Let us adopt the Kubo form for all of the time correlation functions of the frequency fluctuations,

$$\langle\Delta\omega_{ij}(t)\Delta\omega_{kl}(0)\rangle = D_{ij,kl}^2 \exp\left(-t/\tau_{ij,kl}\right), \qquad (23)$$

where $D_{ij,kl}$ and $\tau_{ij,kl}$ are the pre-exponential factor and the time constant of the time-correlation function, respectively. If the frequency fluctuation is in the so-called rapid modulation limit, ($D_{ij,kl}\tau_{ij,kl} \ll 1$), the line-shape function, $g_{ij,kl}(t)$ (Eq. (3)), is equal to $D_{ij,kl}{}^2\tau_{ij,kl}t$. Here, $(1/D_{ij,kl}{}^2\tau_{ij,kl})$ is the vibrational dephasing time, which determines the linewidth of the spectrum.

As an example, we compare the line shape of one diagonal peak at (ω_{ba}, $-\omega_{ba}$) with that of one cross peak at (ω_{ba}, $-\omega_{ca}$). From Eq. 3 the fluctuation terms for the diagonal and cross peaks are expressed as

$$\begin{aligned}
&\left\langle \exp\left\{-i\int_0^{t_1}\Delta\omega_{ab}(\tau)\mathrm{d}\tau - i\int_{t_1}^{t_1+t_2}\Delta\omega_{ba}(\tau)\mathrm{d}\tau\right\}\right\rangle \\
&= \exp\left(-2g_{ab,ab}(t_1) - 2g_{ab,ab}(t_2) + g_{ab,ab}(t_1+t_2)\right), \qquad (24)
\end{aligned}$$

$$\begin{aligned}
&\left\langle \exp\left\{-i\int_0^{t_1}\Delta\omega_{ab}(\tau)\mathrm{d}\tau - i\int_{t_1}^{t_1+t_2}\Delta\omega_{ca}(\tau)\mathrm{d}\tau\right\}\right\rangle \\
&= \exp\big(-g_{ab,ab}(t_1) - g_{ac,ac}(t_2) - g_{ab,ac}(t_1) \\
&\quad - g_{ab,ac}(t_2) + g_{ab,ac}(t_1+t_2)\big) \qquad (25)
\end{aligned}$$

If the time-correlation functions of the frequency fluctuations,

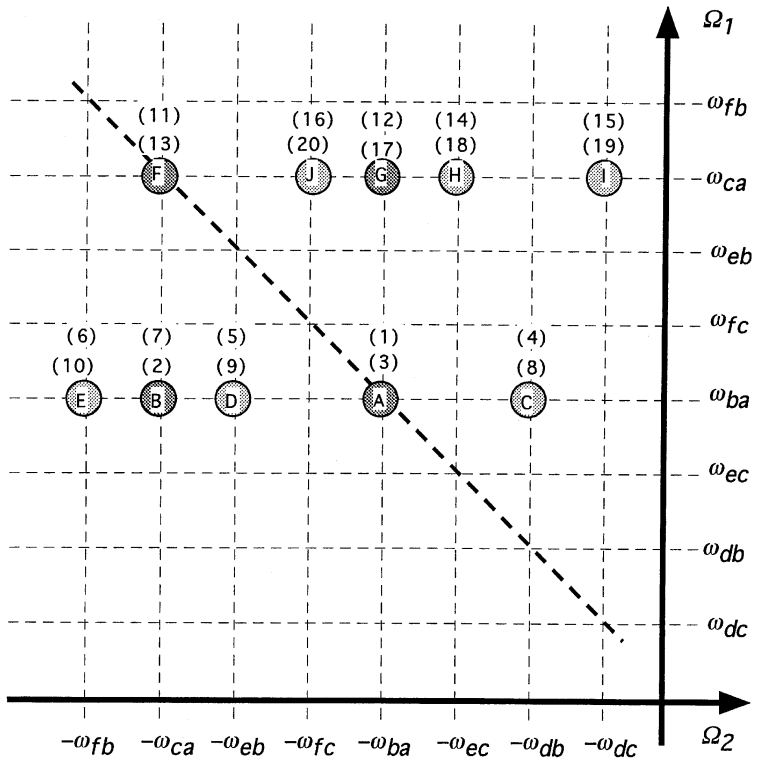

Fig. 3. A schematic picture of the two-dimensional vibrational spectrum for the two vibrational mode case. Each peak is named with a capital alphabet. Numbers in parentheses above the peaks correspond to the diagram in Fig. 2. A sign of the peaks *A*, *B*, *F*, and *G* (indicated with a dark color) is plus, and that of the peaks *C*, *D*, *E*, *H*, *I*, and *J* (indicated with a light color) is minus. A diagonal line is shown for eye guidance.

such as $\langle \Delta\omega_{ba}(t)\Delta\omega_{ba}(0)\rangle$ or $\langle \Delta\omega_{ca}(t)\Delta\omega_{ca}(0)\rangle$, are in the rapid modulation limit, the cross correlation, $\langle \Delta\omega_{ba}(t)\Delta\omega_{ca}(0)\rangle$, is also in the rapid modulation limit, because the magnitudes of the off-diagonal anharmonicities are much smaller than those of the diagonal ones (see Eq. 20 and 21). Therefore, the line-shape functions for the cross correlation in Eq. 25, $-g_{ab,ac}(t_1) - g_{ab,ac}(t_2) + g_{ab,ac}(t_1+t_2)$, can be neglected compared to those for the diagonal terms, $-g_{ab,ab}(t_1) - g_{ac,ac}(t_2)$. Consequently, the time-correlation functions of the cross terms, such as $\langle \Delta\omega_{ba}(t)\Delta\omega_{ca}(0)\rangle$, do not contribute to the response functions of all the 20 quantum pathways very much. Furthermore, if the fluctuations of the frequencies, ω_{ba} and ω_{ca}, are in the rapid modulation limit, the line shape of the cross peak is similar to that of the diagonal peak, since the fluctuation terms for both peaks (Eqs. 24 and 25) are almost identical, This fact indicates

$$\left\langle \exp\left\{-i\int_0^{t_1}\Delta\omega_{ab}(\tau)\mathrm{d}\tau - i\int_{t_1}^{t_1+t_2}\Delta\omega_{ba}(\tau)\mathrm{d}\tau\right\}\right\rangle$$
$$\approx \left\langle \exp\left\{-i\int_0^{t_1}\Delta\omega_{ab}(\tau)\mathrm{d}\tau - i\int_{t_1}^{t_1+t_2}\Delta\omega_{ca}(\tau)\mathrm{d}\tau\right\}\right\rangle$$
$$= \exp\left(-D^2_{ba,ba}\tau_{ba,ba}t_1 - D^2_{ca,ca}\tau_{ca,ca}t_2\right). \quad (26)$$

that the spectral shapes of the diagonal peak at (ω_{ba}, $-\omega_{ba}$) and cross peak at (ω_{ba}, $-\omega_{ca}$) are quite similar.

The double-Fourier transform of Eq. 1 can be easily done in the case of the rapid modulation limit for all frequency fluctuations. If the time dependencies of all eight time-correlation functions for the diagonal terms, such as $\langle \Delta\omega_{ba}(t)\Delta\omega_{ba}(0)\rangle$, are similar, the intensities of the peaks in the 2D spectrum are determined solely by the magnitudes of the transition dipole moment term ($\mu_1\mu_2\mu_3\mu_s$), as can be seen in Eq. 1. If we adopt this assumption for simplicity, all of the peaks, except for the peaks *I* and *E*, have almost equal intensities if cancellation of the peaks does not occur, which is explained in detail in the following section.

3.2. Physical Origin of the Cross Peaks. Peaks *I* and *E* result from the fact that the forbidden transitions for the harmonic oscillator case ($b \rightarrow f$ and $c \rightarrow d$) are allowed due to the presence of anharmonic coupling. Considering the expressions for the transition dipole moment and coefficient of $c_{mn,pq}$, the relative intensities of peaks *I* and *E* with respect to those of the other eight peaks are in the order of $(\gamma_i^3 f_{jkl}/\varepsilon_m)^2$. For ordinary organic molecules, this quantity is on the order of 10^{-2}, at most,[29] suggesting that peaks *E* and *I* are negligibly small compared to the diagonal peaks. Moreover, the optical transitions ($b \rightarrow f$ and $c \rightarrow d$) are allowed even the off-diagonal anharmonicities (f_{112} and f_{122}) are zero, if the diagonal anharmonicities (f_{111} and f_{222}) have finite values. Therefore, the peaks *E* and *I* are not "proper monitors" to investigate the vibrational correlation.

Let us consider the other eight peaks. These eight peaks are categorized into four groups; (*A* and *C*), (*F* and *J*), (*G* and *H*), and (*B* and *D*). Two groups, (*B* and *D*) and (*G* and *H*), disappear if the off-diagonal anharmonicities are zero, because the

corresponding transition frequencies become equal, $\omega_{ca} = \omega_{eb}$ and $\omega_{ba} = \omega_{ec}$, and the peaks have almost equal intensities with opposite signs. In other words, the quantum pathways for the *B* and *D* peaks destructively interfere with each other if the off-diagonal anharmonicities are zero. This cancellation of peaks *B* and *D* is illustrated in Fig. 4. If the anharmonic splitting δ (= $|\omega_{ca} - \omega_{eb}|$) is large enough compared to the linewidth of the peak $\Delta\nu$, the peaks *B* and *D* are well separated, as shown in Figs. 4 (a) and (b). However, if $\delta \ll \Delta\nu$, the two peaks cancels out each other, and the intensity of the resulting peak becomes small ((c) and (d) in Fig. 4). Therefore, the linewidth of the peak as well as the anharmonicity is important for the appearance of the cross peaks (*B* and *D*) and (*G* and *H*). It can be concluded that, different from the peaks *E* and *I*, the cross peaks (*B* and *D*) and (*G* and *H*) carry information about the correlation between the two modes. The other two groups of diagonal peaks (*A* and *C*) and (*F* and *J*) disappear due to destructive interference if the corresponding diagonal anharmonicity is zero. In the case that the two modes are harmonic, no peaks are observed in the spectrum.

Summary

We have theoretically investigated the two-dimensional (2D) vibrational spectra for a two-mode system in terms of a diagrammatic approach. The two vibrational modes are coupled by cubic anharmonicities. The perturbed stationary states are obtained by treating the cubic anharmonicity as a perturbation, and expressions for the third-order response functions are derived. A physical origin of the cross peaks in the 2D spectrum is discussed. There are two different types of cross peaks. One of them results from the anharmonic coupling, carrying information on the vibrational correlation. The vibrational dephasing time is also important for the appearance of the cross peaks. The intensity of the cross peak is almost the same as that of the diagonal peak if the linewidth of the peak is sufficiently small compared to the anharmonic splitting.

Appendix

The other seven expressions for the fluctuations of the transition frequencies are as follows:

$$\hbar\Delta\omega_{ca}(t) = \langle 01|H_c(t)|01\rangle - \langle 00|H_c(t)|00\rangle = \frac{2\gamma_1^2\gamma_2^2 f_{122}}{3\varepsilon_1}F_1(t) + \frac{2\gamma_2^4 f_{222}}{\varepsilon_2}F_2(t) + 2\gamma_2^2 G_{22}(t), \tag{a.1}$$

$$\hbar\Delta\omega_{eb}(t) = \langle 11|H_c(t)|11\rangle - \langle 10|H_c(t)|10\rangle = \hbar\Delta\omega_{fc}(t) = \langle 02|H_c(t)|02\rangle - \langle 01|H_c(t)|01\rangle = \frac{2F_1(t)}{3\varepsilon_1}\gamma_1^2\gamma_2^2 f_{122} + \frac{2F_2(t)}{\varepsilon_2}\gamma_2^4 f_{222} + 2\gamma_2^2 G_{22}(t), \tag{a.2}$$

$$\hbar\Delta\omega_{db}(t) = \langle 20|H_c(t)|20\rangle - \langle 10|H_c(t)|10\rangle = \hbar\Delta\omega_{ec}(t) = \langle 11|H_c(t)|11\rangle - \langle 01|H_c(t)|01\rangle = \frac{2F_1(t)}{\varepsilon_1}\gamma_1^4 f_{111} + \frac{2F_2(t)}{3\varepsilon_2}\gamma_1^2\gamma_2^2 f_{112} + 2\gamma_1^2 G_{11}(t), \tag{a.3}$$

$$\hbar\Delta\omega_{fb}(t) = \langle 02|H_c(t)|02\rangle - \langle 10|H_c(t)|10\rangle = \frac{2\gamma_1^2 F_1(t)}{3\varepsilon_1}\left(-3\gamma_1^2 f_{111} + 2\gamma_2^2 f_{122}\right) + \frac{2\gamma_2^2 F_2(t)}{3\varepsilon_2}\left(-\gamma_1^2 f_{112} + 6\gamma_2^2 f_{222}\right) - 2\gamma_1^2 G_{11}(t) + 4\gamma_2^2 G_{22}(t), \tag{a.4}$$

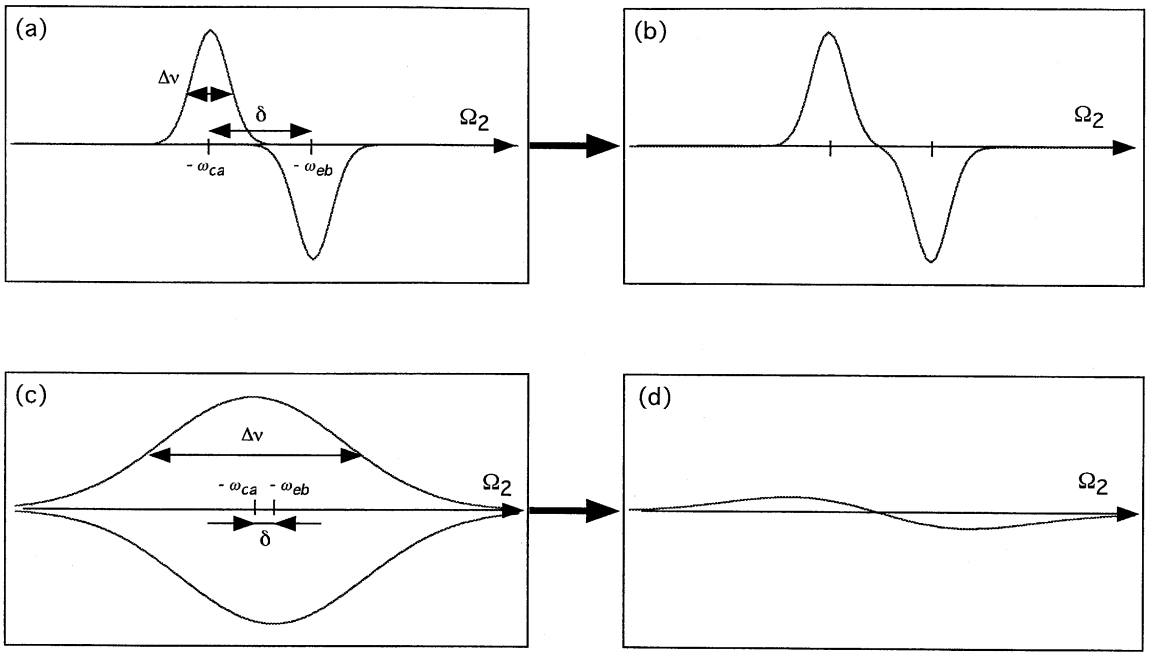

Fig. 4. A schematic picture to illustrate appearance of the cross peaks in the two-dimensional vibrational spectrum. δ and $\Delta\nu$ are the anharmonic splitting and linewidth, respectively. See text in detail.

$$\begin{aligned}\hbar\Delta\omega_{dc}(t) &= \langle 20|H_c(t)|20\rangle - \langle 01|H_c(t)|01\rangle \\ &= \frac{2\gamma_1^2 F_1(t)}{3\varepsilon_1}\left(6\gamma_1^2 f_{111} - \gamma_2^2 f_{122}\right) \\ &\quad + \frac{2\gamma_2^2 F_2(t)}{3\varepsilon_2}\left(2\gamma_1^2 f_{112} - 3\gamma_2^2 f_{222}\right) \\ &\quad + 4\gamma_1^2 G_{11}(t) - 2\gamma_2^2 G_{22}(t). \qquad \text{(a.5)}\end{aligned}$$

This work was partially supported by a grant on Priority Area of "Chemical Reaction Dynamics in Condensed Phases" (10206207) and a grant (10440181) from the Ministry of Education, Science, Sports, and Culture and a JSPS research grant for the Future Program.

References

1 R. F. Loring and S. Mukamel, *J. Chem. Phys.*, **83**, 2116 (1985).

2 X. D. Zhu and Y. R. Shen, *Appl. Phys. B*, **50**, 535 (1990).

3 D. Vanden Bout, L. J. Muller, and M. Berg, *Phys. Rev. Lett.*, **67**, 3700 (1991).

4 P. Guyot-Sionnest, *Phys. Rev. Lett.*, **66**, 1489 (1991).

5 R. Inaba, K. Tominaga, M. Tasumi, K. A. Nelson, and K. Yoshihara, *Chem. Phys. Lett.*, **211**, 183 (1993).

6 Y. Tanimura and S. Mukamel, *J. Chem. Phys.*, **99**, 9496 (1993).

7 V. Khidekel and S. Mukamel, *Chem. Phys. Lett.*, **240**, 304 (1995); V. Chernyak and S. Mukamel, *J. Chem. Phys.*, **108**, 5812 (1998); W. M. Zhang, V. Chernyak and S. Mukamel, *J. Chem. Phys.*, **110** 5011 (1999); S. Mukamel, A. Piryatinski, and V. Chernyak, *J. Chem. Phys.*, **110**, 1711 (1999); S. Mukamel, A. Piryatinski, and V. Chernyak, *Acc. Chem. Res.*, **32**, 145 (1999).

8 J. T. Fourkas, H. Kawashima, and K. A. Nelson, *J. Chem. Phys.*, **103**, 4393 (1995); J. T. Fourkas, *Laser Phys.*, **5**, 656 (1995).

9 K. Tominaga and K. Yoshihara, *Phys. Rev. Lett.*, **74**, 3061 (1996); *J. Chinese Chem. Soc.*, **47**, 631 (2000).

10 T. Steffen and K. Duppen, *Phys. Rev. Lett.*, **76**, 1224 (1996).

11 A. Tokmakoff and G. R. Fleming, *J. Chem. Phys.*, **106**, 2569 (1997).

12 K. Okumura and Y. Tanimura, *J. Chem. Phys.*, **106**, 1687 (1997); *J. Chem. Phys.*, **107**, 2267 (1997); *Chem. Phys. Lett.*, **277**, 159 (1997); *Chem. Phys. Lett.*, **278**, 175 (1997).

13 R. L. Murry and J. T. Fourkas, *J. Chem. Phys.*, **107**, 9726 (1997); R. L. Murry, J. T. Fourkas, and T. Keyes, *J. Chem. Phys.*, **109**, 2814 (1998); *J. Chem. Phys.*, **109**, 7913 (1998).

14 S. Saito and I. Ohmine, *J. Chem. Phys.*, **108**, 240 (1998).

15 M. Cho, *J. Chem. Phys.*, **109**, 5327 (1998); *J. Chem. Phys.*, **111**, 4140 (1999); *J. Chem. Phys.*, **112**, 9978 (2000).

16 J. C. Kirkwood, D. J. Ulness, A. C. Albrecht, and M. J. Stimson, *Chem. Phys. Lett.*, **293**, 417 (1998).

17 J. D. Hybl, A. W. Albrecht, S. M. Gallagher Faeder, and D. M. Jonas, *Chem. Phys. Lett.*, **297**, 307 (1998).

18 D. Blank, L. Kaufman, and G. R. Fleming, *J. Chem. Phys.*, **111**, 3105 (1999).

19 P. Hamm, M. Lim, and R. M. Hochstrasser, *Phys. Rev. Lett.*, **81**, 5326 (1998); M. Lim, P. Hamm, and R. M. Hochstrasser, *Proc. Natl. Acad. Sci. USA*, **95**, 15315 (1998); P. Hamm, M. Lim, W. F. DeGrado, and R. M. Hochstrasser, *Proc. Natl. Acad. Sci. USA*, **96**, 2036 (1999); P. Hamm, M. Lim, W. F. DeGrado, and R. M. Hochstrasser, *J. Chem. Phys.*, **112**, 1907 (2000).

20 W. Zhao and J. C. Wright, *Phys. Rev. Lett.*, **83**, 1950 (1999).

21 M. C. Asplund, M. T. Zanni, and R. M. Hochstrasser, *Proc. Natl. Acad. Sci. USA*, **97**, 8219 (2000).

22 K. Tominaga and H. Meakawa, *J. Luminescence*, **87–89**, 101 (2000); "Proceedings of Two-Dimensional Correlation Spectroscopy," ed by I. Noda and Y. Ozaki, American Institute of Physics (2000), pp. 154–162.

23 R. Ernst, G. Bodenhausen, and A. Wokaun, "Principles of Nuclear Magnetic Resonance in One and Two Dimensions," Clarendon, Oxford, (1987).

24 P. A. Madden and R. M. Lyden-Bell, *Chem. Phys. Lett.*, **38**, 163 (1976).

25 D. W. Oxtoby and S. A. Rice, *Chem. Phys. Lett.*, **42**, 1 (1976).

26 S. Mukamel, "Principles of Nonlinear Optical Spectroscopy," Oxford, New York (1995).

27 C. P. Slichter, "Principles of Magnetic Resonance, 3rd ed.," Springer, Berlin (1996).

28 D. Lee and A. C. Albrecht, in "Advances in Infrared and Raman Spectroscopy," ed by R. J. Clark and R. E. Hester, Wiley–Heydon, New York (1985), Vol. 12.

29 For example, G. Herzberg, "Molecular Spectra and Molecular Structure," Van Nostrand Reinhold, New York (1966).

30 B. T. Darling and D. M. Dennison, *Phys. Rev.*, **57**, 128 (1940).